One-pot Green Synthesis of Carboxylated Cellulose Nanocrystals through Oxidative Degradation of Bamboo Pulp

Linna Lu,[a,b] Yonggui Li,[a,b] Yuanjie Liang,[a] Qin Chen,[a] and Qilin Lu [a,b,]*

Carboxylated cellulose nanocrystals (CCN) were prepared from bamboo pulp by ammonium persulfate (APS) with an ultrasonication-assisted technique. The effects of ultrasonication time, APS concentration, and reaction temperature on the yield of CCN were investigated. The morphology, structure, crystallinity, and thermal properties of prepared samples were analyzed by transmission electron microscopy (TEM), Fourier transform infrared spectroscopy (FTIR), X-ray diffraction (XRD), and thermogravimetric analysis (TGA). The CCN presented rod-like shapes with diameter ranging from 10 to 30 nm and length of 50 to 200 nm. FTIR showed that CCN still kept with the basic chemical structure of cellulose, and at the 1735 cm^{-1} appearing the peak of C=O. The XRD pattern indicated that CCN was characteristic of the cellulose I crystal form, and the crystallinity of CCN was 63%. TGA revealed that CCN had a lower thermal stability than bamboo pulp. This research explored a low-cost and eco-friendly way to prepare CCN.

Keywords: Ammonium persulfate; Ultrasonication-assisted; Carboxylated cellulose nanocrystals; Green processing

*Contact information: a: Clothing and Design Faculty, Minjiang University, Fuzhou 350108, China; b: Fujian Key Laboratory of Novel Functional Textile Fibers and Materials, Minjiang University, Fuzhou 350108, China; *Corresponding author: qilinlu@mju.edu.cn*

INTRODUCTION

Cellulose is the most abundant, renewable, and biodegradable natural polymer on earth (Masruchin *et al.* 2015). The elementary microfibrils contain amorphous and crystalline regions. Cellulose nanocrystals (CNC) can be obtained by removing the amorphous regions of cellulose, leaving the crystalline portions intact. There are various preparation methods such as acid hydrolysis (Tang *et al.* 2014; Yu *et al.* 2019), ion exchange resin hydrolysis (Tang *et al.* 2011), enzymatic hydrolysis (Siqueira *et al.* 2010), and mechanical grinding (Khalil *et al.* 2014). However, acid hydrolysis is the most widely used method for the manufacture of CNC. Sulfuric, hydrochloric, phosphoric, and hydrobromic acids have been used for CNC preparation (Cho and Park 2011; Sadeghifar *et al.* 2011; Yu *et al.* 2013). The diameter of CNC is 5 to 50 nm, and its length ranges from dozens of nanometers to several hundred nanometers (Siró and Plackett 2010). CNC are popular for their low density, high strength, and mechanical and optical properties, which have attracted great interest for their application as reinforcing materials and optical devices (Dufresne 2013).

The major drawback of CNC as reinforcement nanofiber elements is that it aggregates in hydrophobic polymer matrices during compositing processes. The surface modification of cellulose nanocrystals results in more favorable interactions between CNC and hydrophobic matrix polymers in composites to maintain fiber dispersion (Fujisawa *et al.* 2011).

Surface carboxylated nanocrystals can be used directly for further chemical modification. Oxidized cellulose containing carboxylic groups is widely used in medicine to stop bleeding during surgery or to prevent the formation of adhesions following surgery as an important class of biocompatible and bioresorbable products (Follain *et al.* 2008). The increasing carboxyl contents on CNC surface also shows excellent absorbability and flocculation (Song *et al.* 2019). The presence of carboxylic groups improves their dispersion capability in water (Su *et al.* 2014) and provides potential chemical modification for grafting of other radicals onto the cellulose surface (Azzam *et al.* 2010; Barazzouk and Daneault 2012). Furthermore, it can be used as a template to bind different molecules of interest (fluoprobes, antibodies, peptides, *etc.*), thus opening new horizons for various applications of carboxylated cellulose nanocrystals (Follain *et al.* 2010; Barazzouk and Daneault 2011).

Ammonium persulfate (APS) can process a variety of cellulosic biomass without any pretreatments to remove noncellulosic plant contents such as lignin and hemicellulose by a one-pot method. The oxidation only occurs at the hydroxymethyl groups of polysaccharides, while the secondary hydroxyls remained unaffected. APS oxidation method provides a one-step pathway to recycle viscose fiber wastes to nanocelluloses (Ye *et al.* 2018). APS used as an oxidant in aqueous media, but it requires a long reaction time of 16 h (Leung *et al.* 2011; Male *et al.* 2012). In this study, ultrasonication-assisted APS was used to manufacture carboxylated cellulose nanocrystals, which reduced the reaction time to 1 h. Ultrasonication is widely used for catalyzing chemical reactions containing carbohydrate compounds (Mishra *et al.* 2012). Ultrasound energy can be transferred to cellulose chains through cavitation (Lu *et al.* 2015). Ultrasonic cavitation produces intense local heating and high pressure for a very short time, which drives high energy chemical reactions, promoting the mass transfer in inter- and intra-fiber pores (Lu *et al.* 2013; Zhiming *et al.* 2013). The application of ultrasonication in the preparation of CCN may greatly shorten preparation time by accelerating the disintegration of bamboo pulp.

The main goal of this study was to prepare carboxylated cellulose nanocrystals by ammonium persulfate with ultrasonication-assisted treatment. In addition, the morphology, spectroscopic, structure, and thermal properties of the prepared carboxylated cellulose nanocrystals were investigated.

EXPERIMENTAL

Materials and Equipment

Bamboo pulp (94% α-cellulose) was purchased from Nanping Paper Co. Ltd. (Fujian, China). Ammonium persulfate [$(NH_4)_2S_2O_8$, APS] was purchased from Sinopharm Chemical Reagent Beijing Co. Ltd. (Beijing, China). All chemicals were of analytical reagent grade and used without any further purification. The instruments used in the experiments were a KQ-250DB ultrasonic reactor, a DF-101S motor stirrer, a TG16-WS table-top high speed centrifuge and a TD-1B-50 vacuum freeze dryer. A JEM-1010 transmission electron microscope (Japan Electronics Co. Ltd., Tokyo, Japan) was used to investigate the microstructure and size of CCN. The chemical structure of the prepared CCN and BP was performed a Nicolet 380 FTIR spectrometer (Boston, America) with KBr pellets. A Philips-FEI X'Pert Pro MPD X-ray diffractometer (Almelo, Netherlands) was used to investigate the crystal structure and crystallinity index (CrI) of each sample. An NETZSCHSTA449F3 thermal analyzer (Selb, Germany) was used for thermal stability analysis.

Experimental Methods

Manufacture of carboxylated cellulose nanocrystals

First, 2 g of bamboo pulp (BP) was added to 25 mL of certain desired ammonium persulfate concentration (1 to 3 mol/L). The mixing was performed in the ultrasonic reactor at 40 kHz 250 W, 60 to 80 °C for ultrasonication time (1 to 3 h) under continuous stirring at 300 r/min with a poly (tetrafluoroethylene) (PTFE)-coated stirring device. The reacted suspension was washed three times with distilled water by centrifugation (9,000 rpm, 6 min) until the solution pH was neutral. The CCN were collected after five times' repetitive centrifugations at 6,000 rpm for 8 min. The resulting suspension was lyophilized to yield white powder.

Calculation of the CCN yield

The total volume of the prepared CCN suspension was measured. A total of 25 mL of the CCN suspension was transferred to a weighing bottle, followed by freeze-drying. The dried sample was weighed. The yield was calculated according to Eq. 1,

$$\text{Yield}(\%) = \frac{(m_1 - m_2)V_1}{m_3 V_2} \times 100 \tag{1}$$

where m_1 is the total weight of dried CCN and weighting bottle (mg), m_2 is the weight of the weighting bottle (mg), m_3 is the weight of BP (mg), V_1 is the total volume of CCN suspension (mL), and V_2 is the volume of CCN to be dried (mL).

Characterization and Analysis

Transmission electron microscopy (TEM) analysis

The microstructure and size of the CCN was characterized with TEM. A small drop of sample was stained on a carbon-coated grid (400 mesh). The excessive liquid was drained with filter paper followed by staining with phosphotungstic acid. The sample was allowed dried at room temperature and examined using a JEOL JEM-1010 TEM (Japan Electronics Co. Ltd., Japan) at 80 kV.

Fourier-transformed infrared spectra (FTIR) analysis

The chemical structure of the prepared CCN and BP was performed on a Nicolet 380 FTIR spectrometer (Thermo Electron Instruments Co. Ltd., USA) and scanned from 400 to 4,000 cm^{-1} at a resolution of 4 cm^{-1}. KBr pellets were prepared by mixing 1 mg of each sample powder with 150 mg of KBr.

X-ray diffraction (XRD) analysis

The crystal structure and crystallinity index (CrI) of each sample was investigated on an X'Pert Pro MPD X-ray diffractometer (Philips-FEI, Netherlands) with Cu Kα radiation at wavelength λ = 0.154 nm in the range 2θ = 6° to 90° at a speed of 0.1°/s.

The crystallinity index (CrI) of cellulose samples was calculated from the X-ray diffraction patterns by Eq. 2 (Segal *et al.* 1959),

$$\mathrm{CrI} = \frac{I_{002} - I_{am}}{I_{002}} \times 100 \tag{2}$$

where I_{002} is the diffracted intensity of the crystalline segments at the peak about 2θ = 22° and I_{am} is the diffracted intensity of the amorphous regions at about 2θ = 18°.

Thermal characterization

The samples were ground into powder and mounted on a holder. Thermal stability analysis of each sample was characterized by thermal analyzer (NETZSCHSTA449F3, Germany). Under N_2 atmosphere, the heating temperature ranged from 25 to 600 ℃ at a fixed heating rate of 10 ℃/min.

RESULTS AND DISCUSSION

Effects of Reaction Conditions on the Yield of CCN

Results and analysis of variance

The main influence factors on the yield of CCN are ultrasonication time, APS concentration, and reaction temperature. Figure 1a shows the effect of ultrasonication time on the yield of CCN. At APS concentration of 2 mol/L and reaction temperature of 70 ℃, the yield of CCN increased from 27% to 46% when the ultrasonication time increased from 1 h to 2 h. With the increased ultrasonication time, more ultrasound energy is transferred to cellulose chains during the process of cavitation. Consequently, the amorphous region is destroyed, and cellulosic macromolecules disintegrate into nanosize. However, the yield decreased to 37% when the ultrasonication time increased to 3 h. The decrease in yield at longer ultrasonication time suggested that crystalline regions were destroyed partially.

Figure 1b shows the effect of APS concentration on the yield of CCN. When ultrasonication time was 2 h and reaction temperature was 70 ℃, the yield of CCN reached 46% with the APS concentration increasing to 2 mol/L. The result is attributed to the increasing sulfate radicals and hydrogen peroxide decomposed by APS, which accelerates the disintegration of amorphous regions to obtain more CCN. Increasing the concentration to 3 mol/L decreased the yield to 26%. This result was attributed to the destruction of the crystalline regions of cellulose by excess sulfate radicals and hydrogen peroxide.

Figure 1c shows the effect of reaction temperature on the yield of CCN. At an ultrasonication time of 2 h and APS concentration of 2 mol/L, the yield of CCN increased from 36.35% to 46.41% with the reaction temperature increasing from 60 ℃ to 70 ℃.

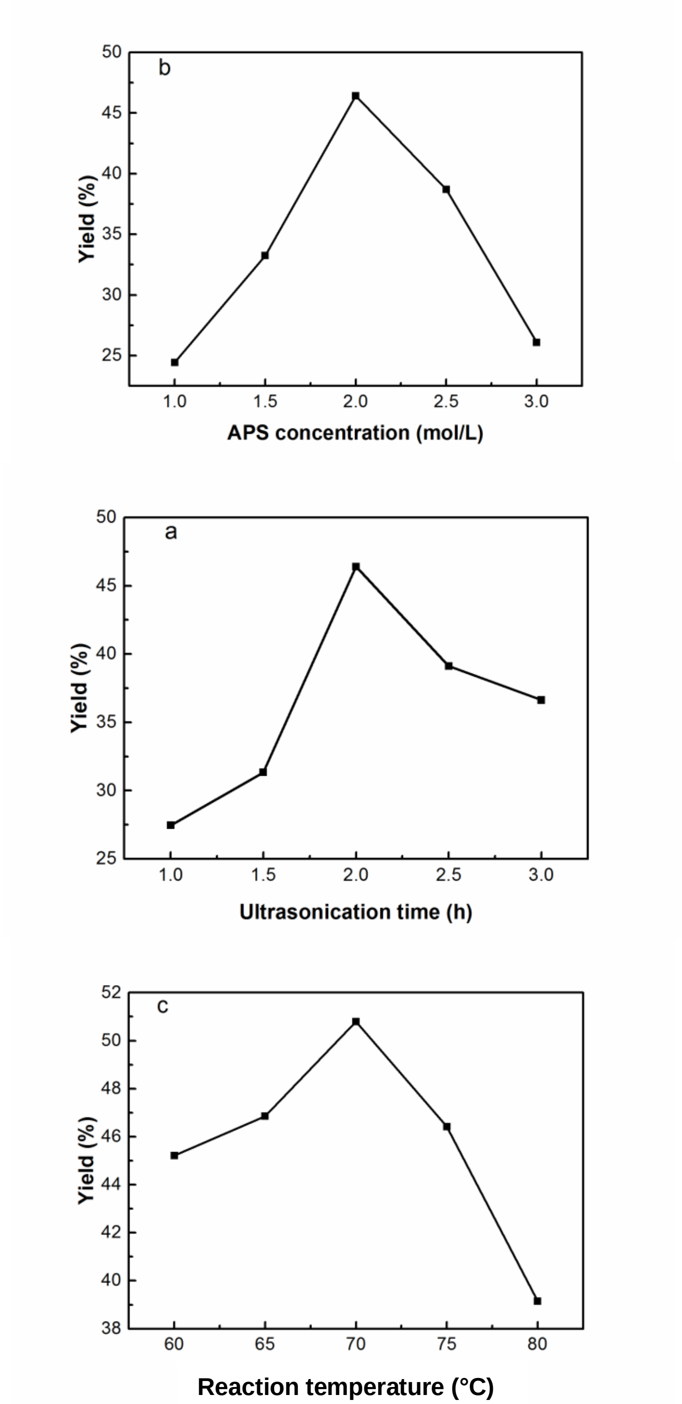

Fig. 1. Effect of (a) ultrasonication time, (b) reaction time, and (c) APS concentration on the yield of CCN

This result indicates that the decomposition speed of APS increased with increasing temperature, generating more sulfate radicals and hydrogen peroxide during the oxidation process. However, when the reaction temperature increased to 80 °C, the yield decreased to 28%. The decreased yield of CCN at high reaction temperature may be due to the rapid decomposition of ammonium persulfate, weakening the disintegration of cellulose.

CCN Characteristics

TEM analysis

Figure 2 shows the TEM image of CCN. The CCN particles present a short rod-like shape with diameters ranging from 10 to 30 nm and lengths of 50 to 200 nm. As the oxidation of cellulose by APS mainly occurred on the hydroxyl group of C6, so the formed CCN remained large amount of hydroxyl groups, which leads to some aggregation of CCN due to interfacial hydrogen bonds. However, the agglomeration is less than that of hydrochloric acid method because of the large electrostatic repulsion between nanocrystals due to the existence of carboxyl groups. The size distribution curves of CCN from TEM images are shown in Fig. 3.

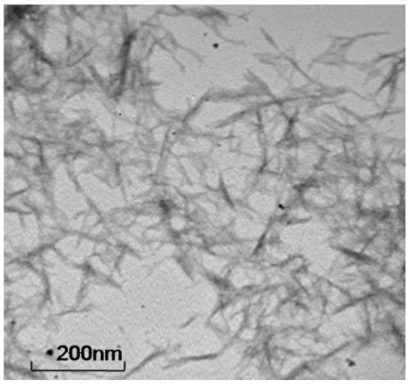

Fig. 2. TEM image of CCN

The reaction parameters have effects on the CCN size and the size distribution of CCN under different reaction parameters is shown in Table 1.

Table 1. Size Distribution of CCN under Different Reaction Parameters

Ultrasonication time (h)	Reaction temperature (˚C)	APS concentration (mol/L)	Length (nm)	Width (nm)
1	70	2	212	47
2	70	2	100	15
3	70	2	56	9
2	70	1	166	27
2	70	1.5	120	23
2	70	2.5	78	10
2	60	2	203	32
2	75	2	113	28
2	80	2	92	8

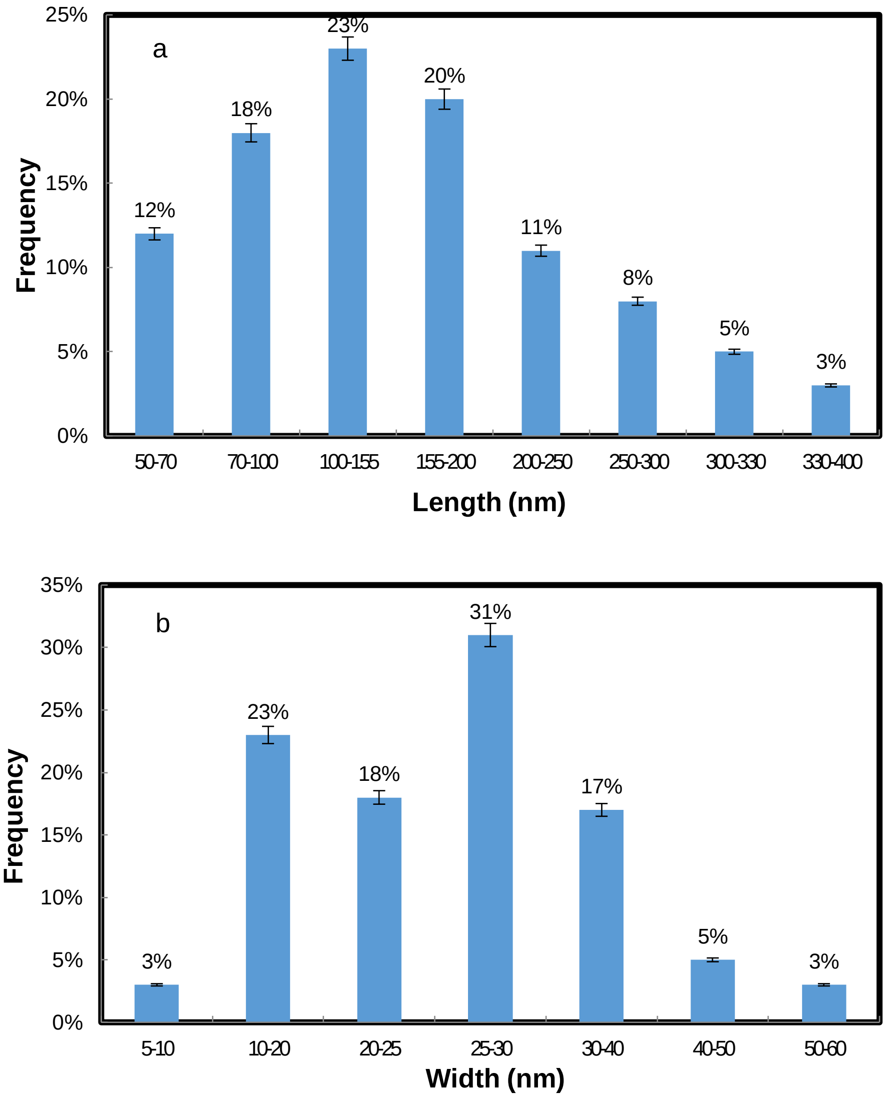

Fig. 3. (a) Length and (b) Width distributions of CCN

FTIR spectroscopy analysis

The FTIR spectra of BP and CCN are presented in Fig. 4. The absorbance peaks at 3353, 2898, 1434, 1382, and 895 cm^{-1} are associated with cellulose I. Chemical structures of the two samples are represented as follows. The primary peaks at 3,353 cm^{-1} and 2,898 cm^{-1} are assigned to O-H stretching and C-H stretching vibration, respectively. The band at 1,640 cm^{-1} is related to the vibration of adsorbed water due to the presence of abundant hydrophilic hydroxide radical in the cellulose (Alemdar and Sain 2008). The band at 1,382 cm^{-1} reflects C-H asymmetric deformations (Sun *et al.* 2005). Absorption at 1,060 cm^{-1} is indicative of C-O stretching vibrations (Xiao *et al.* 2001). The band at 895 cm^{-1} is assigned the β-glycosidic linkages between glucose units in cellulose (Oh *et al.* 2005). Compared with the FTIR spectrum of BP, a new absorption peak at 1,735 cm^{-1} corresponds to the

C=O stretching frequency of carboxylic acid groups, indicating the success of the carboxylation.

The degree of oxidation (DO) and content of carboxylic acid groups of CCN were measured by conductometric titration (Wang *et al.* 2018; Yu *et al.* 2016), and the calculated DO and carboxyl content of CCN were 0.127 and 0.87 mmol/g, respectively.

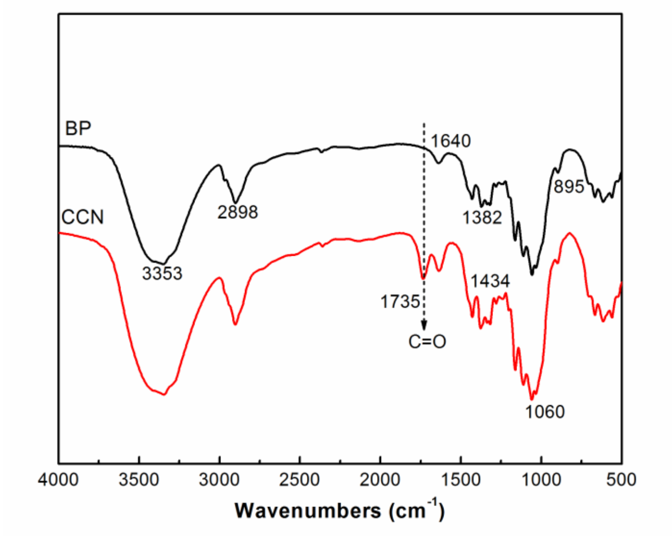

Fig. 4. FTIR spectrum of BP and CCN

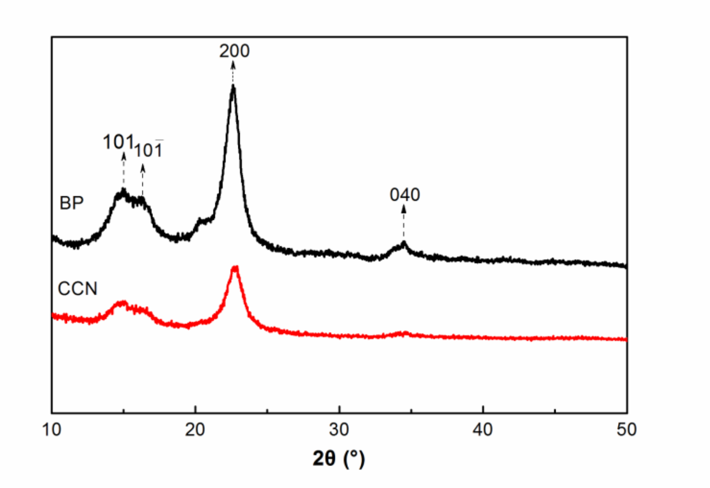

Fig. 5. XRD patterns of BP and CCN

X-ray diffraction measurements

To elucidate the structural changes caused by APS treatment, X-ray diffraction analysis was conducted, as shown in Fig. 5. Both samples displayed the typical X-ray diffraction pattern of cellulose I. The main diffraction peaks at 2θ values of 15.3°, 16.2°, 22.5°, and 34.5° were assigned to the 101, $10\bar{1}$, 200 and 040 diffraction planes, respectively (Liu *et al.* 2010; Sèbe *et al.* 2012). The crystallinity of cellulose nanocrystals (CNC) obtained by sulfuric acid hydrolysis was also calculated, and the results showed that the crystallinity of CNC prepared by sulfuric acid hydrolysis was 79.3%; however, the crystallinity of CCN prepared by APS decreased to 63%. The decrease in crystallinity reflects that part of the crystalline structure of cellulose was damaged during oxidation with APS.

Thermal stability analysis

The TGA and DTG curves of BP and CCN are shown in Fig. 6. The slight weight loss below 100 °C was due to water evaporation in the samples. The initial thermal decomposition of BP was 338.5 °C, which was higher than that at 256.5 °C for CCN. This lower degradation temperature for CCN could be due to partial hydrolysis of crystalline regions during oxidation. The maximum weight loss of thermal decomposition peaks for BP and CCN appeared at 363.8 °C and 325.6 °C, respectively. The results indicate that CCN presents a lower thermal stability during oxidation.

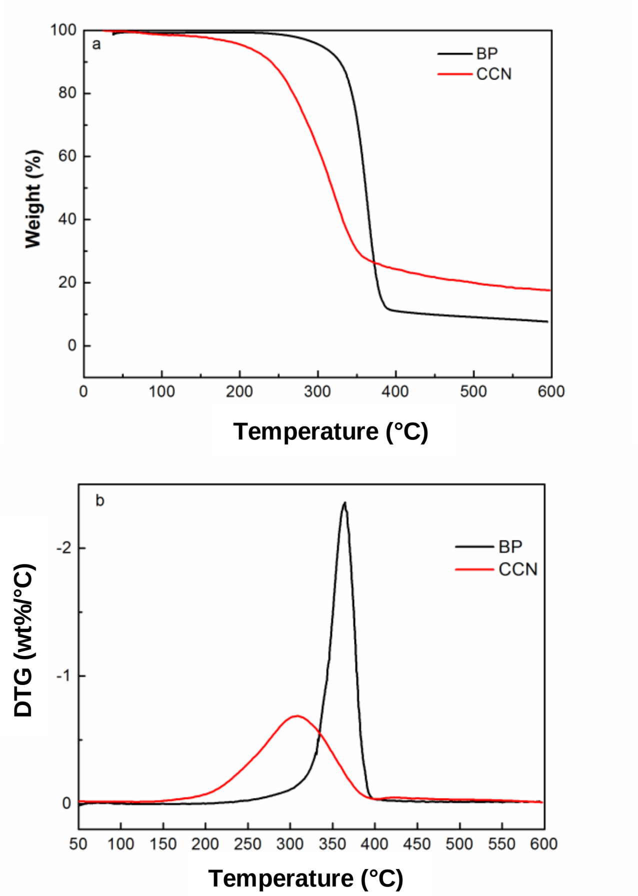

Fig. 6. (a) TG and (b) DTG curves of BP and CCN

CONCLUSIONS

1. Carboxylated cellulose nanocrystals were synthesized *via* APS oxidative degradation of bamboo pulp under ultrasound assistance.
2. The combination of ultrasonication and APS oxidation created mechanochemical

synergy to disintegrate cellulose into CCN, which avoided the tedious separation of intermediate products.

3. Ultrasonication-assisted treatment played an important role in facilitating the oxidation of bamboo for manufacturing CCN. The main factors of ultrasonication time, APS concentration, and reaction temperature on the yield of CCN were investigated, and a yield of 46% was obtained.
4. The manufactured CCN presented a short rod-like shape with diameters ranging from 10 to 30 nm and lengths of 50 to 200 nm.

ACKNOWLEDGMENTS

The authors appreciate the generous financial support of the Open Project Program of Fujian Key Laboratory of Novel Functional Textile Fibers and Materials, Minjiang University, China, Grant No. FKLTFM1703, FKLTFM1803; Fujian Middle-aged and Young Teacher Education Research Project, Grant No. JT180389; Science and Technology Project of Fuzhou City, Grant No. 2019-S-63; Open Project Program of Key Laboratory of National Forestry & Grassland Bureau for Plant Fiber Functional Materials, Fujian Agriculture and Forestry University, Grant No. 2019KFJJ01 and Talent Introduction Program of Minjiang University, Grant No. MJY18010.

REFERENCES CITED

Alemdar, A., and Sain, M. (2008). "Isolation and characterization of nanofibers from agricultural residues – Wheat straw and soy hulls," *Bioresource Technology* 99(6), 1664-1671. DOI: 10.1016/j.biortech.2007.04.029

Azzam, F., Heux, L., Putaux, J. L., and Jean, B. (2010). "Preparation by grafting onto, characterization, and properties of thermally responsive polymer-decorated cellulose nanocrystals," *Biomacromolecules* 11(12), 3652-3659. DOI: 10.1021/bm101106c

Barazzouk, S., and Daneault, C. (2011). "Spectroscopic characterization of oxidized nanocellulose grafted with fluorescent amino acids," *Cellulose* 18(3), 643-653. DOI: 10.1007/s10570-011-9503-5

Barazzouk, S., and Daneault, C. (2012). "Tryptophan-based peptides grafted onto oxidized nanocellulose," *Cellulose* 19(2), 481-493. DOI: 10.1007/s10570-011-9633-9

Cho, M. J., and Park, B. D. (2011). "Tensile and thermal properties of nanocellulose-reinforced poly (vinyl alcohol) nanocomposites," *Journal of Industrial and Engineering Chemistry* 17(1), 36-40. DOI: 10.1016/j.jiec.2010.10.006

Dufresne, A. (2013). "Nanocellulose: A new ageless bionanomaterial," *Materials Today* 16(6), 220-227. DOI: 10.1016/j.mattod.2013.06.004

Follain, N., Marais, M. F., Montanari, S., and Vignon, M. R. (2010). "Coupling onto surface carboxylated cellulose nanocrystals," *Polymer* 51(23), 5332-5344. DOI: 10.1016/j.polymer.2010.09.001

Follain, N., Montanari, S., Jeacomine, I., Gambarelli, S., and Vignon, M. R. (2008). "Coupling of amines with polyglucuronic acid: Evidence for amide bond formation," *Carbohydrate Polymers* 74(3), 333-343. DOI: 10.1016/j.carbpol.2008.02.016

Fujisawa, S., Okita, Y., Saito, T., Togawa, E., and Isogai, A. (2011). "Formation of N-acylureas on the surface of TEMPO-oxidized cellulose nanofibril with carbodiimide in DMF," *Cellulose* 18(5), 1191. DOI: 10.1007/s10570-011-9578-z

Khalil, H. A., Davoudpour, Y., Islam, M. N., Mustapha, A., Sudesh, K., Dungani, R., and Jawaid, M. (2014). "Production and modification of nanofibrillated cellulose using various mechanical processes: A review," *Carbohydrate Polymers* 99, 649-665. DOI: 10.1016/j.carbpol.2013.08.069

Leung, A. C., Hrapovic, S., Lam, E., Liu, Y., Male, K. B., Mahmoud, K. A., and Luong, J. H. (2011). "Characteristics and properties of carboxylated cellulose nanocrystals prepared from a novel one-step procedure," *Small* 7(3), 302-305. DOI: 10.1002/smll.201001715

Liu, D., Zhong, T., Chang, P. R., Li, K., and Wu, Q. (2010). "Starch composites reinforced by bamboo cellulosic crystals," *Bioresource Technology* 101(7), 2529-2536. DOI: 10.1016/j.biortech.2009.11.058

Lu, Q., Lin, W., Tang, L., Wang, S., Chen, X., and Huang, B. (2015). "A mechanochemical approach to manufacturing bamboo cellulose nanocrystals," *Journal of Materials Science* 50(2), 611-619. DOI: 10.1007/s10853-014-8620-6

Lu, Z., Fan, L., Zheng, H., Lu, Q., Liao, Y., and Huang, B. (2013). "Preparation, characterization and optimization of nanocellulose whiskers by simultaneously ultrasonic wave and microwave assisted," *Bioresource Technology* 146, 82-88. DOI: 10.1016/j.biortech.2013.07.047

Male, K. B., Leung, A. C., Montes, J., Kamen, A., and Luong, J. H. (2012). "Probing inhibitory effects of nanocrystalline cellulose: Inhibition *versus* surface charge," *Nanoscale* 4(4), 1373-1379. DOI: 10.1039/C2NR11886F

Masruchin, N., Park, B. D., Causin, V., and Um, I. C. (2015). "Characteristics of TEMPO-oxidized cellulose fibril-based hydrogels induced by cationic ions and their properties," *Cellulose* 22(3), 1993-2010. DOI: 10.1007/s10570-015-0624-0

Mishra, S. P., Manent, A. S., Chabot, B., and Daneault, C. (2012). "Production of nanocellulose from native cellulose-various options utilizing ultrasound," *BioResources* 7(1), 0422-0436. DOI: 10.1080/02773813.2011.624668

Oh, S. Y., Yoo, D. I., Shin, Y., Kim, H. C., Kim, H. Y., Chung, Y. S., Park, W. H., and Youk, J. H. (2005). "Crystalline structure analysis of cellulose treated with sodium hydroxide and carbon dioxide by means of X-ray diffraction and FTIR spectroscopy," *Carbohydrate Research* 340(15), 2376-2391. DOI: 10.1016/j.carres.2005.08.007

Sadeghifar, H., Filpponen, I., Clarke, S. P., Brougham, D. F., and Argyropoulos, D. S. (2011). "Production of cellulose nanocrystals using hydrobromic acid and click reactions on their surface," *Journal of Materials Science* 46(22), 7344-7355. DOI: 10.1007/s10853-011-5696-0

Sèbe, G., Ham-Pichavant, F., Ibarboure, E., Koffi, A. L. C., and Tingaut, P. (2012). "Supramolecular structure characterization of cellulose II nanowhiskers produced by acid hydrolysis of cellulose I substrates," *Biomacromolecules* 13(2), 570-578. DOI: 10.1021/bm201777j

Segal, L. G. J. M. A., Creely, J. J., Martin Jr, A. E., and Conrad, C. M. (1959). "An empirical method for estimating the degree of crystallinity of native cellulose using the X-ray diffractometer," *Textile Research Journal* 29(10), 786-794. DOI: 10.1177/004051755902901003

Siqueira, G., Tapin-Lingua, S., Bras, J., da Silva Perez, D., and Dufresne, A. (2010). "Morphological investigation of nanoparticles obtained from combined mechanical shearing, and enzymatic and acid hydrolysis of sisal fibers," *Cellulose* 17(6), 1147-1158. DOI: 10.1007/s10570-010-9449-z

Siró, I., and Plackett, D. (2010). "Microfibrillated cellulose and new nanocomposite materials: A review," *Cellulose* 17(3), 459-494. DOI: 10.1007/s10570-010-9405-y

Song, M. L., Yu, H. Y., Chen, L. M., Zhu, J. Y., Wang, Y. Y., Yao, J. M., Zhou, Z., and Tam, K. C. (2019). "Multibranch strategy to decorate carboxyl groups on cellulose nanocrystals to prepare adsorbent/flocculants and pickering emulsions," *ACS Sustainable Chemistry & Engineering* 7(7), 6969-6980. DOI: 10.1021/acssuschemeng.8b06671

Sun, X. F., Xu, F., Sun, R. C., Fowler, P., and Baird, M. S. (2005). "Characteristics of degraded cellulose obtained from steam-exploded wheat straw," *Carbohydrate Research* 340(1), 97-106. DOI: 10.1016/j.carres.2004.10.022

Su, Y., Burger, C., Hsiao, B. S., and Chu, B. (2014). "Characterization of TEMPO-oxidized cellulose nanofibers in aqueous suspension by small-angle X-ray scattering," *Journal of Applied Crystallography* 47(2), 788-798. DOI: 10.1107/S1600576714005020

Tang, L. R., Huang, B., Ou, W., Chen, X. R., and Chen, Y. D. (2011). "Manufacture of cellulose nanocrystals by cation exchange resin-catalyzed hydrolysis of cellulose," *Bioresource Technology* 102(23), 10973-10977. DOI: 10.1016/j.biortech.2011.09.070

Tang, Y., Yang, S., Zhang, N., and Zhang, J. (2014). "Preparation and characterization of nanocrystalline cellulose via low-intensity ultrasonic-assisted sulfuric acid hydrolysis," *Cellulose* 21(1), 335-346. DOI: 10.1007/s10570-013-0158-2

Wang, D., Yu, H., Fan, X., Gu, J., Ye, S., Yao, J., and Ni, Q. (2018). "High aspect ratio carboxylated cellulose nanofibers cross-linked to robust aerogels for superabsorption–flocculants: paving way from nanoscale to macroscale," *ACS Applied Materials & Interfaces* 10(24), 20755-20766. DOI: 10.1021/acsami.8b04211

Xiao, B., Sun, X., and Sun, R. (2001). "Chemical, structural, and thermal characterizations of alkali-soluble lignins and hemicelluloses, and cellulose from maize stems, rye straw, and rice straw," *Polymer Degradation and Stability* 74(2), 307-319. DOI: 10.1016/S0141-3910(01)00163-X

Ye, S., Yu, H., Wang D., Zhu, J., and Gu., J. (2018). "Green acid-free one-step hydrothermal ammonium persulfate oxidation of viscose fiber wastes to obtain carboxylated spherical cellulose nanocrystals for oil/water Pickering emulsion," *Cellulose* 25(9), 5139-5155. DOI: 10.1007/s10570-018-1917-x

Yu, H., Abdalkarim, S., Y., H., Zhang, H., Wang, C., Tam, K., C., (2019). "Simple process to produce high-yield cellulose nanocrystals using recyclable citric/hydrochloric acids," *ACS Sustainable Chemistry & Engineering* 7(5), 4912-4923. DOI:10.1021/acssuschemeng.8b05526

Yu, H., Qin, Z., Liang, B., Liu, N., Zhou, Z., and Chen, L. (2013). "Facile extraction of thermally stable cellulose nanocrystals with a high yield of 93% through hydrochloric acid hydrolysis under hydrothermal conditions," *Journal of Materials Chemistry A*

1(12), 3938-3944. DOI: 10.1039/C3TA01150J

Yu, H., Y., Zhang, D. Z., Lu, F. F., and Yao, Ju. (2016). "New approach for single-step extraction of carboxylated cellulose nanocrystals for their use as adsorbents and flocculants," *ACS Sustainable Chemistry & Engineering* 4(5), 2632-2643. DOI: 10.1021/acssuschemeng.6b00126

Zhiming, L., Haiying, W., Wei, M., and Cheng, X. (2013). "Preparation optimization and characterization of reed pulp nanocrystalline cellulose with ultrasonic methods," *Chinese Wild Plant Resources* 32(02), 15-19. DOI: 10.3969/j.issn.1006-9690.2013.02.005

Article submitted: July 21, 2019; Peer review completed: September 3, 2019; Revised version received and accepted: November 4, 2019; Published: November 8, 2019.
DOI: 10.15376/biores.15.1.49-61